Grip and slip of L1-CAM on adhesive substrates direct growth cone haptotaxis

Kouki Abe[a,1], Hiroko Katsuno[a,1], Michinori Toriyama[a], Kentarou Baba[a], Tomoyuki Mori[b], Toshio Hakoshima[b], Yonehiro Kanemura[c], Rikiya Watanabe[d], and Naoyuki Inagaki[a,2]

[a]Laboratory of Systems Neurobiology and Medicine, Graduate School of Biological Sciences, Nara Institute of Science and Technology, Ikoma 630-0192, Japan; [b]Laboratory of Structural Biology, Graduate School of Biological Sciences, Nara Institute of Science and Technology, Ikoma 630-0192, Japan; [c]Division of Regenerative Medicine, Institute for Clinical Research, Department of Neurosurgery, Osaka National Hospital, National Hospital Organization, Osaka 540-0006, Japan; and [d]Department of Applied Chemistry, Graduate School of Engineering, University of Tokyo, Tokyo 113-8656, Japan

Edited by Vann Bennett, Duke University Medical Center, Durham, NC, and approved January 19, 2018 (received for review June 30, 2017)

Chemical cues presented on the adhesive substrate direct cell migration, a process termed haptotaxis. To migrate, cells must generate traction forces upon the substrate. However, how cells probe substrate-bound cues and generate directional forces for migration remains unclear. Here, we show that the cell adhesion molecule (CAM) L1-CAM is involved in laminin-induced haptotaxis of axonal growth cones. L1-CAM underwent grip and slip on the substrate. The ratio of the grip state was higher on laminin than on the control substrate polylysine; this was accompanied by an increase in the traction force upon laminin. Our data suggest that the directional force for laminin-induced growth cone haptotaxis is generated by the grip and slip of L1-CAM on the substrates, which occur asymmetrically under the growth cone. This mechanism is distinct from the conventional cell signaling models for directional cell migration. We further show that this mechanism is disrupted in a human patient with L1-CAM syndrome, suffering corpus callosum agenesis and corticospinal tract hypoplasia.

cell migration | cell adhesion | axon guidance | clutch | shootin1

Cell migration toward proper destinations is an essential step in multiple biological processes such as embryogenesis, axon guidance, immune responses, and tissue regeneration. Cell migration can be directed by extracellular chemical cues such as soluble chemicals (called chemotaxis) and substrate-bound chemicals (termed haptotaxis), and haptotaxis is thought to be a major mode of directional cell migration in tissues (1–4). For understanding directional cell migration, it is essential to identify the molecular mechanism by which cells generate forces to migrate toward their destinations. In classical models of haptotaxis, chemical cues on the substrate are proposed to act as ligands that activate receptors on the membrane (2, 5). However, despite recent progress in identifying molecules and signaling pathways (6–8), how cells generate directional forces for haptotaxis remains unclear.

The growth cone located at the tip of extending axons senses external chemical cues and plays key roles in axon outgrowth and guidance (2). Actin filament (F-actin) networks polymerize at the leading edge of motile cells and disassemble proximally (2, 9, 10), which, in conjunction with myosin II activity, induces retrograde flow of F-actins (10, 11). Mechanical coupling between the F-actin retrograde flow and cell adhesion molecules by "clutch" molecules transmits the force of F-actin flow to the substrate, thereby generating the traction force required for growth cone migration (2, 10, 12). We previously reported that shootin1 (13), recently renamed shootin1a (14), and cortactin (15) function as clutch molecules (16, 17): They couple the F-actin retrograde flow and the transmembrane cell adhesion molecule (CAM) L1-CAM (18, 19), producing traction force on the substrate for growth cone migration. In addition, a previous study reported frictional slippage (20, 21) of the CAM integrin on the substrates (22) and suggested its involvement in focal adhesion maturation (22). However, the potential roles of the frictional slippage of CAMs on the substrates remain largely unknown.

Laminins are major components of the extracellular matrix (19, 23) that bind to various adhesion molecules, including L1-CAM (19, 24–26). Laminins function as attractive chemical cues for haptotaxis of axonal growth cones (27–29), while L1-CAM is involved in axon outgrowth and guidance in vitro and in vivo (30–32). We have analyzed the molecular mechanics underlying laminin-induced haptotaxis of axonal growth cones and show that the F-actin retrograde flow, L1-CAM, shootin1a, and cortactin are involved in the laminin-induced haptotaxis. We propose that the directional force for haptotaxis is generated by grip and slip of L1-CAM on the substrates, which occur asymmetrically under the growth cone, and show that this mechanism is disrupted in a human patient of L1-CAM or corpus callosum hypoplasia, retardation, adducted thumbs, spastic paraplegia, and hydrocephalus (CRASH) syndrome.

Results

Myosin II, F-Actin Retrograde Flow, L1-CAM, Shootin1a, and Cortactin Are Involved in the Laminin-Induced Growth Cone Haptotaxis. To analyze the molecular mechanics underlying laminin-induced growth cone haptotaxis, we prepared microscale patterns of laminin on polylysine-coated coverslips (Fig. 1*A* and Fig. S1 *A* and *B*). Neurons can extend their axons either on laminin or polylysine, but prefer laminin (27). Time-lapse imaging showed that axonal growth cones of cultured rat hippocampal neurons dynamically search for substrates, thereby preferentially migrating along laminin-coated pathways (Fig. 1*A* and Movie S1). F-actins polymerize at the leading edge of growth cones and disassemble proximally (2, 10); this, together with myosin II activity, induces

Significance

Cell migration directed by substrate-bound chemical cues is called haptotaxis. This study shows that grip and slip between the cell adhesion molecule (CAM) L1-CAM and the adhesive substrates, which occur asymmetrically under the growth cone, direct growth cone migration mediated by laminin. This mechanism is disrupted in a human patient of L1-CAM syndrome, suffering corpus callosum agenesis and corticospinal tract hypoplasia. These findings provide a conceptual framework for understanding the regulation and dysregulation of cell migration on the bases of force generation.

Author contributions: K.A., T.M., T.H., Y.K., R.W., and N.I. designed research; K.A., H.K., M.T., and K.B. performed research; K.A., H.K., and K.B. analyzed data; and K.A., H.K., R.W., and N.I. wrote the paper.

The authors declare no conflict of interest.

This article is a PNAS Direct Submission.

[1]K.A. and H.K. contributed equally to this work.

[2]To whom correspondence should be addressed. Email: ninagaki@bs.naist.jp.

This article contains supporting information online at www.pnas.org/lookup/suppl/doi:10.1073/pnas.1711667115/-/DCSupplemental.

Published online February 26, 2018.

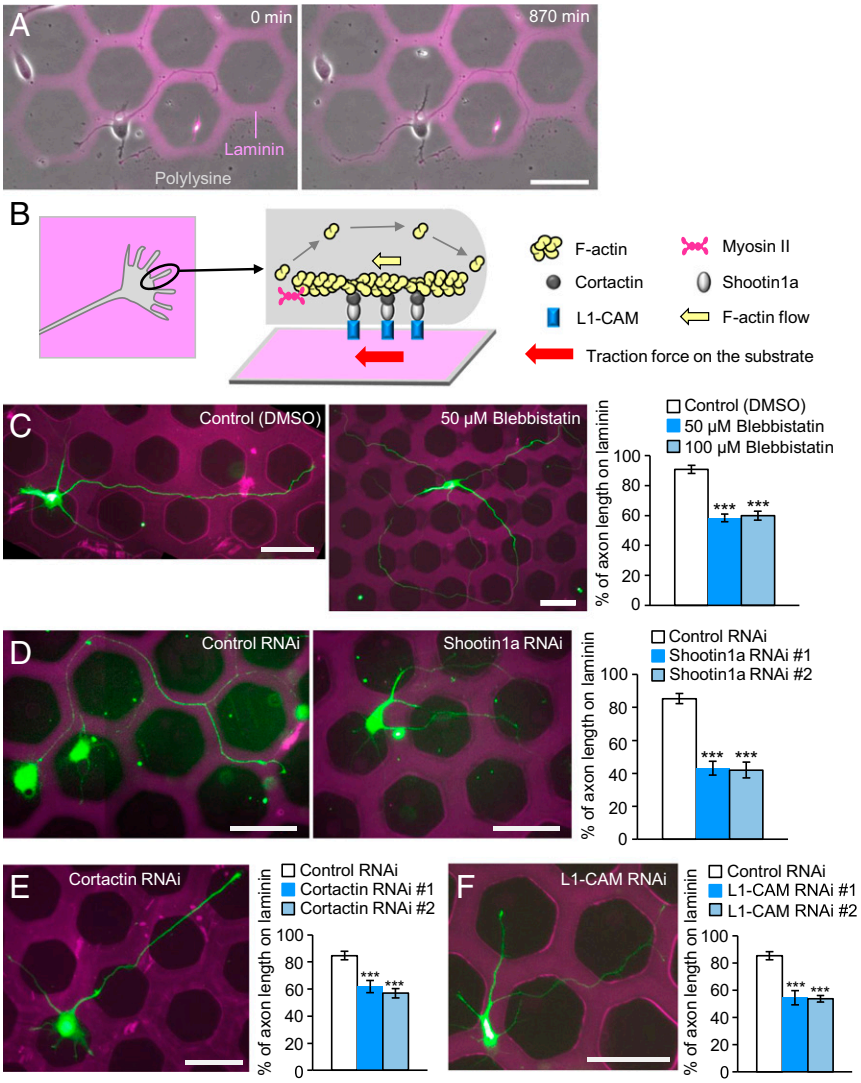

Fig. 1. Involvement of F-actin retrograde flow, shootin1a, cortactin, and L1-CAM in laminin-induced axonal haptotaxis. (*A*) Time-lapse images of a hippocampal neuron cultured on a microscale pattern of laminin and polylysine during day in vitro (DIV) 1 to 2 (Movie S1). (*B*) A diagram showing F-actin, myosin II, cortactin, shootin1a, and L1-CAM at the leading edge of an axonal growth cone. (*C*) Hippocampal neurons treated with DMSO, 50 μM blebbistatin, or 100 μM blebbistatin were cultured on microscale patterns of laminin (pink) and polylysine (black) for 3 d and stained with an anti-βIII-tubulin antibody (green). The graph shows the percentage of axon length located on laminin ($n = 90$ neurons). (*D*, *E*, and *F*) Hippocampal neurons transfected with control miRNA or the expression vector for (*D*) shootin1a miRNA, (*E*) cortactin miRNA, or (*F*) L1-CAM miRNA were cultured on microscale patterns of laminin (pink) and polylysine (black) for 3 d. Green color is the signal of EGFP. The graphs show the percentage of axon length located on laminin; $n = 72$ neurons in *D*, 97 neurons in *E*, and 74 neurons in *F*; #1 and #2 indicate RNAi with miRNA #1 and #2, respectively. Data in *C*–*F* represent means ± SEM; $***P < 0.01$. (Scale bars: 50 μm.)

F-actin retrograde flow (yellow arrow, Fig. 1*B*) (10, 11). On the other hand, shootin1a and cortactin couple the F-actin flow and L1-CAM as clutch molecules, producing traction force on the substrate for growth cone migration (red arrow, Fig. 1*B*) (16, 17). Consistent with a previous report (28), in the presence of the myosin II inhibitor blebbistatin (50 μM or 100 μM), axons frequently crossed the borders between laminin and polylysine and extended onto both substrates (Fig. 1*C*). Similar data were obtained by inhibiting actin polymerization with 1 μM cytochalasin D (Fig. S1*D*). In addition, suppression of shootin1a (Fig. 1*D*), cortactin (Fig. 1*E*), or L1-CAM (Fig. 1*F*) by RNAi significantly decreased the ratio of axons which extended on laminin. We reported previously that the amino acid residues 261 to 377 of shootin1a act as a dominant negative mutant (DN) that disrupts the interaction between shootin1a and cortactin, thereby inhibiting the coupling between F-actins and the adhesive substrate (17). Overexpression of shootin1a DN disturbed laminin-mediated growth cone haptotaxis (Fig. S1*E*), indicating that the clutch coupling mediated by shootin1a–cortactin interaction is required for laminin-mediated growth cone haptotaxis. Together, these results suggest that the molecular machinery composed of myosin II, retrogradely flowing F-actin, shootin1a, cortactin, and L1-CAM (Fig. 1*B*) is involved in laminin-induced growth cone haptotaxis.

Laminin Promotes Traction Force Generated by Growth Cones. To analyze the molecular mechanics underlying laminin-induced axonal haptotaxis, we next measured traction force generated by axonal growth cones. Neurons were cultured on polyacrylamide gels coated with polylysine alone (polylysine) or polylysine plus laminin (laminin); 200-nm fluorescent beads were also embedded in the gels. Traction force under the axonal growth cones was monitored by visualizing force-induced deformation of the elastic gel, which is reflected by displacement of the beads from their original positions. As reported previously (17, 21), the reporter beads under the growth cones moved dynamically (Fig. 2 *A* and *B* and Movie S2), and the net force produced by the growth cones was oriented toward the rear of the growth cones as noted by the angle of averaged stress near 0 (Fig. 2*C*). The magnitude of the traction force produced on the polylysine-coated substrate was 2.1 ± 0.4 pN/μm^2 (mean ± SEM, $n = 11$ growth cones) (Fig. 2*C*). On the other hand, the magnitude of the force produced on the laminin-coated substrate was 8.2 ± 2.2 pN/μm^2 ($n = 14$ growth cones), and significantly greater than that produced on polylysine (Fig. 2*C*).

Laminin Reduces the Retrograde Flow Speeds of F-Actin and Shootin1a in Growth Cones. To elucidate the molecular mechanism by which the growth cone produces greater force on laminin than on polylysine, we analyzed actin dynamics in growth cones by monitoring mRFP-actin expressed in hippocampal neurons. As reported (21, 33), F-actin retrograde flow was observed at the leading edge of axonal growth cones as retrogradely moving fluorescent features

CELL BIOLOGY

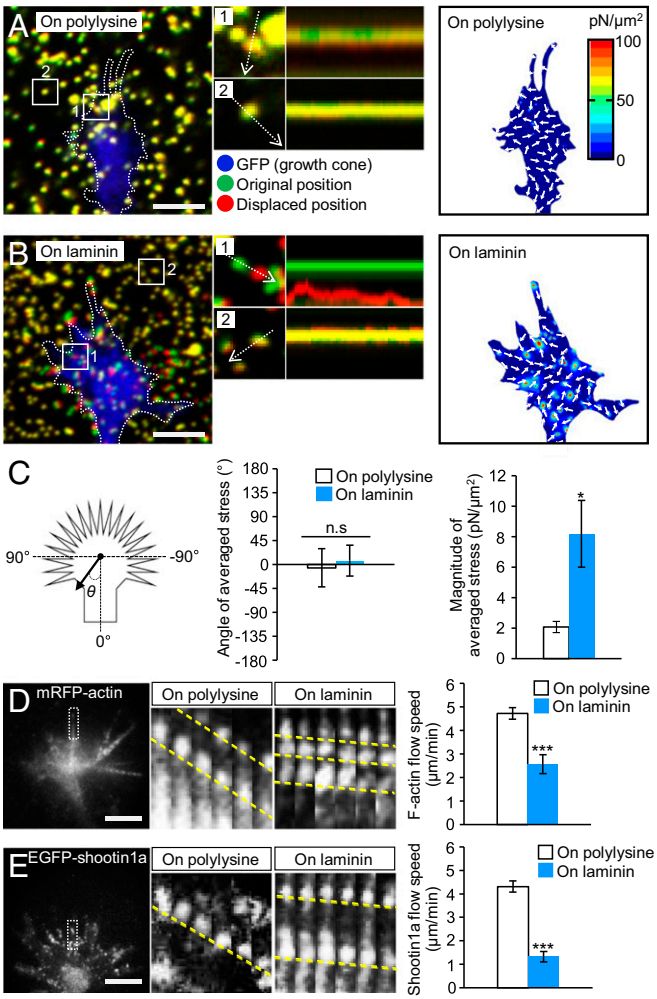

Fig. 2. Laminin on the adhesive substrate promotes traction force and reduces retrograde flow of F-actin and shootin1a at growth cones. (*A* and *B*) (*Left*) Fluorescence images showing axonal growth cones of DIV1 neurons expressing GFP and cultured on (*A*) polylysine-coated or (*B*) laminin-coated polyacrylamide gel with embedded 200-nm fluorescent beads. The pictures show representative images from time-lapse series taken every 3 s for 147 s (Movie S2). The original and displaced positions of the beads in the gel are indicated by green and red colors, respectively. Dashed lines indicate the boundary of the growth cones. (*Middle*) The kymographs along the axis of bead displacement (white dashed arrows) at the indicated areas 1 and 2 of the growth cone show movement of beads recorded every 3 s. The bead in area 2 is a reference bead. (*Right*) The stress maps during the initial 30-s observations. (*C*) Statistical analyses of the angle (θ) and magnitude of the traction forces under axonal growth cones on polylysine-coated or laminin-coated polyacrylamide gel; $n = 25$ growth cones. The magnitude of the force produced on the laminin-coated substrate was significantly greater than that produced on polylysine, while the angles of the forces on polylysine and laminin were not statistically different from 0. (*D* and *E*) (*Left*) Fluorescent feature images of (*D*) mRFP-actin and (*E*) EGFP-shootin1a at axonal growth cones cultured on polylysine. (*Middle*) Kymographs of the fluorescent features of mRFP-actin and EGFP-shootin1a in filopodia on polylysine (boxed area) and laminin at 5-s intervals are shown (F-actin and shootin1a flows are indicated by dashed yellow lines) (Movies S3 and S4). (*Right*) Graphs show retrograde flow rates obtained from the kymograph analyses ($n =$ 607 signals in *D* and 805 signals in *E*). Data in *D* and *E* represent means ± SEM; $*P < 0.05$; $***P < 0.01$; ns, nonsignificant. (Scale bars: 5 μm.)

of mRFP-actin (Fig. 2*D* and Movie S3). On the polylysine-coated substrate, F-actins in growth cones moved retrogradely at 4.7 ± 0.2 μm/min (mean ± SEM, $n = 301$ signals). On the other hand, F-actins showed retrograde movement at 2.6 ± 0.4 μm/min ($n = 306$ signals) in the growth cones on the laminin-coated substrates; the speed of F-actin flow was significantly slower on laminin than on polylysine (Fig. 2*D*). Similar data for F-actin flow were reported recently using *Xenopus* spinal neurons (34). Consistent with the report that the clutch molecule shootin1a interacts with F-actin retrograde flow through cortactin (Fig. 1*B*) (17), EGFP-shootin1a expressed in hippocampal neurons underwent retrograde flow in the growth cones (Fig. 2*E* and Movie S4); the speed of shootin1a flow was also significantly slower on laminin than on polylysine. A previous report proposed that laminin stimulates myosin II contractile activity, thereby causing laminin-induced growth cone haptotaxis (28). We consider that this mechanism does not play a dominant role here, because the stimulation of myosin II is associated with an increase in F-actin retrograde flow speed (Fig. S2 *A* and *C*) (11), whereas the present case is accompanied by decreases in the flow speeds of F-actin and shootin1a (Fig. 2 *D* and *E* and Fig. S2*C*).

L1-CAM in Growth Cones Undergoes Grip and Slip on the Substrates. To further analyze the mechanism for laminin-mediated axonal haptotaxis, we next monitored the movement of L1-CAM, which is linked to the F-actin flow through shootin1a and cortactin (Fig. 1*B*), in the growth cone membrane. L1-CAM-HaloTag expressed in hippocampal neurons was labeled by tetramethylrhodamine (TMR) ligand and observed by total internal reflection fluorescence (TIRF) microscopy (Fig. 3*A* and Movie S5). Two types of L1-CAM signals were observed: immobile L1-CAM puncta (pink dashed lines, Fig. 3*A*) and retrogradely flowing L1-CAM puncta (blue dashed lines). We also observed signals that stopped and then flowed and vice versa, suggesting that the same molecules switch between these stop and flow phases. On polylysine, 22% of L1-CAM signals displayed stop phase and 78% displayed flow phase ($n = 1{,}076$ phases, 235 signals), while 51% of the signals stopped and 49% flowed on laminin ($n = 1{,}531$ phases, 268 signals) (Fig. S3*A*). The percentage of the stop phase was significantly larger on laminin than on polylysine (Fig. S3*A*). The durations of the stop phase of L1-CAM on laminin and on polylysine were not statistically different (Fig. S3*B*). Consistent with these data, the mean flow speed of L1-CAM was slower on laminin (Fig. S3*C*). A previous study reported that integrin linked to F-actin retrograde flow undergoes frictional slippage on the substrate (22). As observed in the case of integrin (22), we found that the traction force under the growth cone correlated inversely with the flow speed of L1-CAM: An increase in the traction force on laminin (Fig. 2*C*) is accompanied by a decrease in the L1-CAM flow speed (Fig. 3*D* and Figs. S2*C* and S3*C*). It has been reported that promotion of the mechanical coupling between F-actin flow and L1-CAM by cell signaling decreases the F-actin flow rate and increases the traction force (17, 33). However, we consider that an increase in F-actin–L1-CAM coupling does not occur here, because it would increase the L1-CAM flow rate (Fig. S2 *B* and *C*), whereas the present case is accompanied by a decrease of the flow rate (Figs. S2*C* and S3*C*). To demonstrate directly that the slippage occurs mainly between L1-CAM and the substrate, not between F-actin flow and L1-CAM, we monitored F-actin flow and L1-CAM flow in the growth cones simultaneously (Fig. S3*D* and Movies S6 and S7). F-actins and L1-CAM flowed at similar rates, which were significantly slower on laminin than on polylysine (Fig. S3*E*), indicating that the slippage occurs mainly between L1-CAM and the substrate. Together, these results indicate that L1-CAM switches between two adhesive states: L1-CAM that is immobilized (grip) and that undergoes slippage (slip) on the substrate, and that ratio of the grip state increases on laminin.

Grip and Slip Model for Laminin-Induced Growth Cone Haptotaxis. To examine whether such differential grip and slip states occur within single growth cones, L1-CAM movement was analyzed in growth cones located on the border between laminin and polylysine (Fig. 3*B* and Movie S8). As shown in Fig. 3 *B* and *C*, the

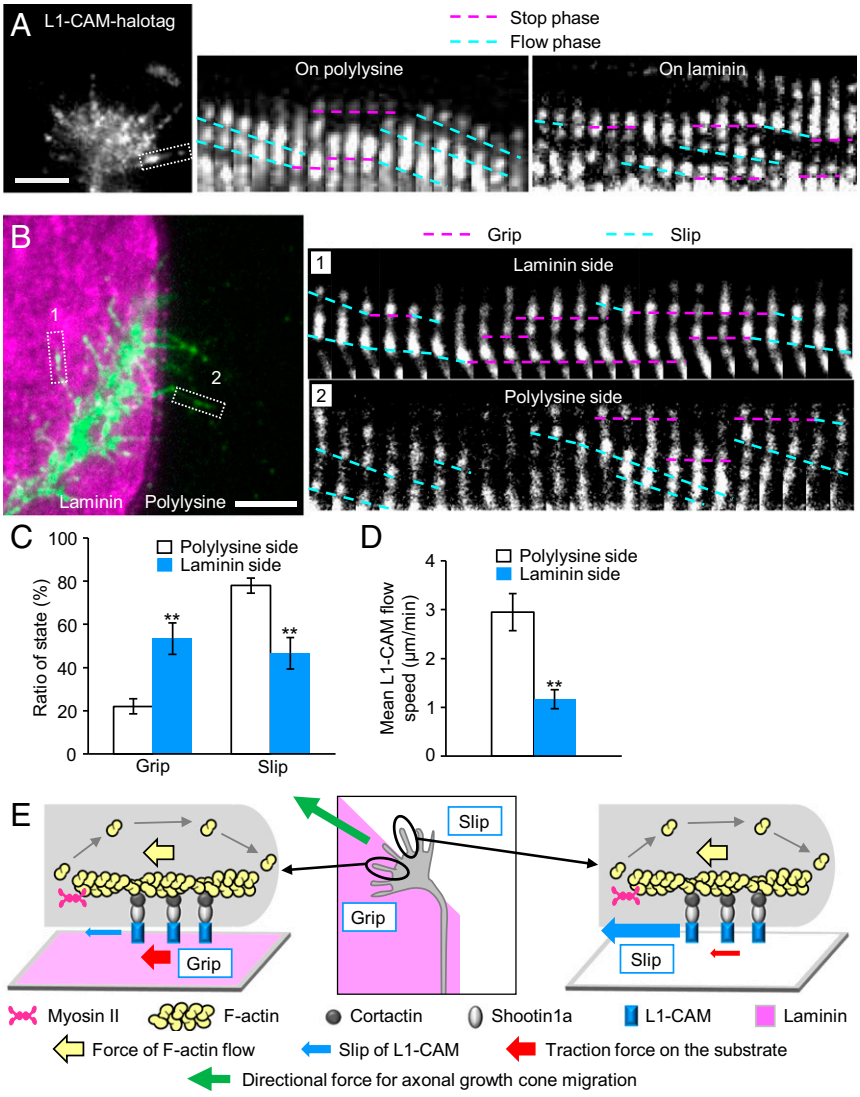

Fig. 3. L1-CAM in the growth cone membrane undergoes grip and slip on the adhesive substrates. (*A*) A fluorescent feature image of L1-CAM-HaloTag at an axonal growth cone cultured on polylysine. Kymographs of the fluorescent features of L1-CAM-HaloTag in filopodia on polylysine (boxed area) and laminin at 5-s intervals are shown (stop and flow phases are indicated by dashed pink and blue lines, respectively) (Movie S5). (*B*) A fluorescent feature image of L1-CAM-HaloTag at an axonal growth cone located on the laminin/polylysine border. Kymographs of the fluorescent features of L1-CAM-HaloTag in filopodia on polylysine and laminin (boxed areas) at 5-s intervals are shown (grip and slip states are indicated by dashed pink and blue lines, respectively) (Movie S8). (*C*) Ratio of the grip and slip states and (*D*) retrograde flow speed of L1-CAM-HaloTag in filopodia obtained from the kymograph analyses in *B*; $n = 334$ signals. (*E*) Grip and slip model for laminin-induced growth cone haptotaxis. The force of actin filament flow in the growth cone (yellow arrows) is transmitted through cortactin, shootin1a, and L1-CAM to the substrate (red arrows). L1-CAM undergoes grip or frictional slip on the adhesive substrates. Larger numbers of L1-CAM molecules undergo grip on the laminin side than on the control substrate side, allowing for more efficient transmission of the force on the laminin side (red arrows). This asymmetric grip and slip of L1-CAM within a growth cone generates directional force for growth cone haptotaxis toward laminin (green arrow). Data in *C* and *D* represent means ± SEM; $^{**}P < 0.02$. (Scale bars: 5 μm.)

percentage of the grip state was significantly larger on the laminin side of the growth cones, while that of the slip state was larger on the polylysine side. Consistent with these observations, the mean flow speed of L1-CAM was significantly slower on the laminin side than on the polylysine side (Fig. 3*D*). These findings led us to propose a mechanism by which growth cones generate directional force for laminin-induced axonal haptotaxis (Fig. 3*E*). The force of F-actin flow (yellow arrows) is transmitted to the substrate (red arrows) through cortactin, shootin1a, and L1-CAM (17). As laminin interacts specifically with L1-CAM (25, 26), while polylysine alone permits L1-CAM-independent cell adhesion, laminin presents a more adhesive substrate for L1-CAM than polylysine, as observed here (Fig. 3 *A*–*D*). Thus, within a growth cone on the laminin–polylysine border, larger numbers of L1-CAM molecules are in the grip state on the laminin side in comparison with the polylysine side, allowing for more efficient transmission of the force on the laminin side (red arrows, Fig. 3*E*). These differential grip and slip states within a growth cone generate directional force for axonal haptotaxis toward laminin (green arrow).

Axonal Haptotaxis Mediated by the Grip and Slip Mechanism Is Disrupted in a Human Patient of L1-CAM/CRASH Syndrome. Mutations in human L1-CAM gene cause X-linked disorders called L1-CAM syndrome or CRASH syndrome, with characteristic symptoms: corpus callosum hypoplasia, mental retardation, adducted thumbs, spastic paraplegia, and hydrocephalus (19, 24, 35). Finally, we analyzed L1-CAM from a patient having this syndrome in which Thr273 of the extracellular domain (ECD) is deleted (L1-CAM-ΔT273) (35, 36). The patient was aborted in the 21st week of gestation, suffering corpus callosum agenesis, corticospinal tract hypoplasia, hydrocephalus, and adducted thumb (35, 36). To examine the behavior of L1-CAM-ΔT273 in axonal growth cones, neurons were cotransfected with an L1-CAM miRNA, which reduces the endogenous L1-CAM level, and RNAi-refractory L1-CAM-HaloTag (ΔT273). Control experiments were performed using RNAi-refractory L1-CAM-HaloTag [wild-type (WT)].

As shown in Fig. 4 *A* and *B* (see also Movie S9), the grip state of L1-CAM-ΔT273 on laminin was significantly lower than that of L1-CAM-WT, concurrent with its increased retrograde flow velocity (Fig. 4*C*). The ΔT273 mutation also increased the retrograde flow speed of shootin1a on laminin (Fig. 4*D*). Consequently, the significant differences in the percentage of grip and slip states of L1-CAM-WT observed on laminin and on polylysine were lost in L1-CAM-ΔT273 (Fig. 4*B*), and the duration of the stop phase of L1-CAM was reduced by ΔT273 mutation (Fig. S3*F*), thereby indicating that the deletion of Thr273 in L1-CAM leads to dysfunction of the differential grip and slip mechanism. Consistent with the decreased grip state of L1-CAM-ΔT273 on

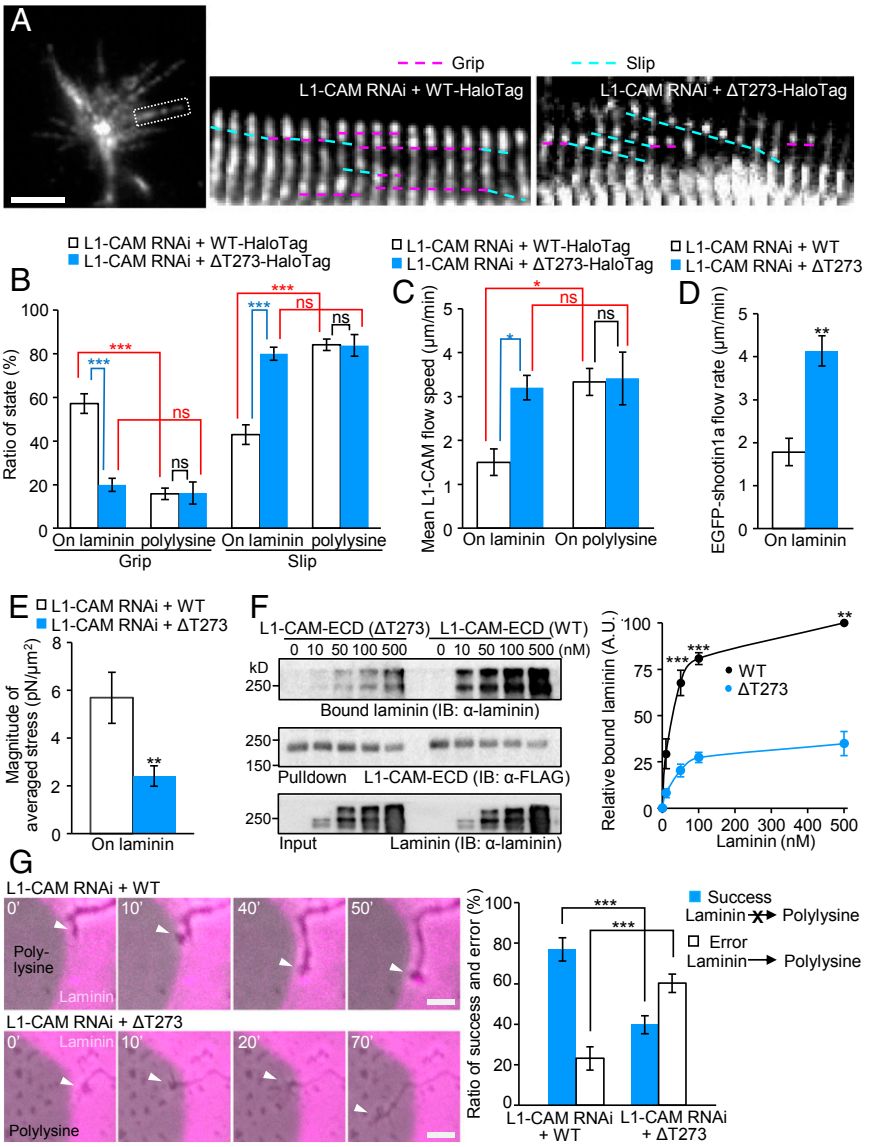

Fig. 4. Deletion of Thr273 in L1-CAM leads to dysfunction of the differential grip mechanism and disrupts laminin-induced axonal haptotaxis. (*A*) Neurons coexpressing L1-CAM miRNA and RNAi-refractory L1-CAM-HaloTag (WT or ΔT273) were cultured on laminin, and fluorescent features of L1-CAM-HaloTag were analyzed. Kymographs of the fluorescent features of L1-CAM-HaloTag in filopodia on laminin (boxed area) at 5-s intervals are shown (grip and slip phases are indicated by dashed pink and blue lines, respectively) (Movie S9). (*B*) Ratio of the grip and slip states and (*C*) retrograde flow speed of L1-CAM-HaloTag in filopodia obtained from the kymograph analyses in *A* (n = 904 signals). (*D*) Neurons coexpressing L1-CAM miRNA, RNAi-refractory L1-CAM-HaloTag (WT or ΔT273) and EGFP-shootin1a were cultured on laminin, and fluorescent features of EGFP-shootin1a were analyzed. (*E*) Neurons coexpressing L1-CAM miRNA and RNAi-refractory L1-CAM-EGFP (WT or ΔT273) were cultured on laminin-coated polyacrylamide gel. The magnitude of the traction forces under axonal growth cones was quantified and statistically analyzed. (*F*) (*Left*) In vitro binding assay using purified laminin and purified FLAG-His-tagged L1-CAM-ECD (WT or ΔT273). L1-CAM-ECD (WT or ΔT273) at increasing concentrations was incubated with laminin and Ni-nitrilotriacetic acid (Ni-NTA) agarose beads. L1-CAM-ECD was eluted. After SDS/PAGE, the eluate was immunoblotted with anti-laminin and anti-FLAG antibodies, and the bound laminin was then quantified (*Right*). Data represent means ± SEM (n = 3). (*G*) (*Left*) Time-lapse images of growth cones (arrowheads) coexpressing L1-CAM miRNA and RNAi-refractory L1-CAM-EGFP (WT or ΔT273) cultured on microscale patterns of laminin (pink) and polylysine (gray) (Movie S10). (*Right*) The graph shows the percentages of the growth cones that did not cross the border from laminin to polylysine successfully and those that exited from laminin to polylysine in error (n = 110 growth cones). Data in *B*–*G* represent means ± SEM; *P < 0.05; **P < 0.02; ***P < 0.01; ns, nonsignificant. (Scale bars: 5 μm for *A* and 10 μm for *G*.)

laminin (Fig. 4*B* and Fig. S3*F*), this mutation decreased significantly the magnitude of the traction force produced on laminin (Fig. 4*E*). An in vitro binding assay demonstrated that the ΔT273 mutation also reduced the interaction between L1-CAM ECD and laminin (Fig. 4*F*), suggesting that the decreased grip state of L1-CAM-ΔT273 on laminin results from its reduced interaction with the substrate.

Finally, we analyzed the effect of the ΔT273 mutation on laminin-mediated axonal haptotaxis. Expression of RNAi-refractory L1-CAM rescued the L1-CAM RNAi-induced reduction of the ratio of axons that extended on laminin (74% rescue, Fig. 1*F* and Fig. S4*A*). On the other hand, the rescue of the ratio was significantly reduced when RNAi-refractory L1-CAM-ΔT273 was expressed (Fig. S4*A*). In addition, time-lapse imaging showed that the majority (77%) of the growth cones expressing WT L1-CAM did not cross the border from laminin to polylysine successfully, while the remainder (23%) exited from laminin to polylysine in error (Fig. 4*G* and Movie S10). Importantly, the error ratio was

significantly increased by the Thr273 deletion (Fig. 4*G*), indicating that the mutation disrupts laminin-induced axonal haptotaxis. The ΔT273 mutation did not have a significant effect on growth cone exit from polylysine to laminin (Fig. S4*B*). Together, these data not only demonstrate a linkage between L1-CAM syndrome and the differential grip and slip mechanism, but also correlate functionally the differential grip and slip states (Fig. 4 *A* and *B*) and laminin-induced axonal haptotaxis (Fig. 4*G* and Fig. S4*A*).

Discussion

This study proposes a mechanical model of haptotaxis in which differential grip and slip of L1-CAM on the substrates direct growth cone migration (Fig. 3*E*). A previous study on fish keratocytes proposed two mechanisms for F-actin retrograde flow that have distinct effects on traction force (37). One is slippage between CAMs and substrates, where the adhesion substrate slip positively correlates with traction force; this mechanism is compatible with the signaling model in which receptor activation promotes actin polymerization or myosin II activation (Fig. S2*A*) (28). The other is slippage between F-actin flow and CAMs; this corresponds to the classic slip clutch mechanism, which can be also regulated by cell signaling (Fig. S2*B*) (10, 33, 34). On the other hand, our data on growth cones showed a slippage between L1-CAM and substrates and demonstrated a negative correlation between the L1-CAM slippage and force generation (Figs. 2*C* and 3 *A*–*D*). The present model (Fig. 3*E*) is distinct from the above two models (Fig. S2 *A* and *B*): L1-CAM acts as both a chemosensor and a mechano-effector for generating directional force to drive growth cone migration. In addition, dysfunction of this mechanism is associated with L1-CAM syndrome. L1-CAM also interacts with CAMs, such as L1-CAM itself, axonin-1/TAG-1, F3/F11/contactin, and DM1-GRASP as well as the extracellular matrix component phosphacan (19, 25), raising the possibility that the grip and slip mechanism may be involved not only in extracellular matrix-based but also in cell–cell contact-based growth cone migration (38). In addition, L1-CAM is associated with cancer metastasis as well as with L1-CAM syndrome (24, 39). Because of its potential versatility, the present mechanism may also account for haptotaxis mediated by other CAMs on the basis of force generation.

Methods

Cell culture, transfection, preparation of microscale patterns of laminin on polylysine-coated coverslips, RNAi, DNA constructs, immunocytochemistry, immunoblot, microscopy, analysis of axons located on microscale patterns of laminin and polylysine, fluorescent speckle microscopy, traction force microscopy, protein preparation, in vitro binding assay, and statistical analysis are described in detail in *SI Methods*. All relevant aspects of the experimental procedures were approved by the Institutional Animal Care and Use Committee of Nara Institute of Science and Technology.

ACKNOWLEDGMENTS. We thank Dr. V. Lemmon for providing L1-CAM constructs and Dr. Y. Sakumura for discussion. This research was supported in part by a Japan Society for the Promotion of Science (JSPS) Grant-in-Aid for Scientific Research on Innovative Areas (JP25102010, to N.I.), JSPS KAKENHI (JP23370088 and JP26290007, to N.I.), Japan Agency for Medical Research and Development (AMED) under Grant JP17gm0810011 (to N.I., T.H., and Y.K.), the Osaka Medical Research Foundation for Incurable Diseases (N.I. and M.T.), and the Takeda Science Foundation (T.H. and N.I.).

1. Carter SB (1967) Haptotaxis and the mechanism of cell motility. *Nature* 213:256–260.
2. Lowery LA, Van Vactor D (2009) The trip of the tip: Understanding the growth cone machinery. *Nat Rev Mol Cell Biol* 10:332–343.
3. Varadarajan SG, et al. (2017) Netrin1 produced by neural progenitors, not floor plate cells, is required for axon guidance in the spinal cord. *Neuron* 94:790–799.e3.
4. Dominici C, et al. (2017) Floor-plate-derived netrin-1 is dispensable for commissural axon guidance. *Nature* 545:350–354.
5. Maness PF, Schachner M (2007) Neural recognition molecules of the immunoglobulin superfamily: Signaling transducers of axon guidance and neuronal migration. *Nat Neurosci* 10:19–26.
6. Wu C, et al. (2012) Arp2/3 is critical for lamellipodia and response to extracellular matrix cues but is dispensable for chemotaxis. *Cell* 148:973–987.
7. San Miguel-Ruiz JE, Letourneau PC (2014) The role of Arp2/3 in growth cone actin dynamics and guidance is substrate dependent. *J Neurosci* 34:5895–5908.
8. Johnson HE, et al. (2015) F-actin bundles direct the initiation and orientation of lamellipodia through adhesion-based signaling. *J Cell Biol* 208:443–455.
9. Pollard TD, Borisy GG (2003) Cellular motility driven by assembly and disassembly of actin filaments. *Cell* 112:453–465.
10. Suter DM, Forscher P (2000) Substrate-cytoskeletal coupling as a mechanism for the regulation of growth cone motility and guidance. *J Neurobiol* 44:97–113.
11. Medeiros NA, Burnette DT, Forscher P (2006) Myosin II functions in actin-bundle turnover in neuronal growth cones. *Nat Cell Biol* 8:215–226.
12. Mitchison T, Kirschner M (1988) Cytoskeletal dynamics and nerve growth. *Neuron* 1:761–772.
13. Toriyama M, et al. (2006) Shootin1: A protein involved in the organization of an asymmetric signal for neuronal polarization. *J Cell Biol* 175:147–157.
14. Higashiguchi Y, et al. (2016) Identification of a shootin1 isoform expressed in peripheral tissues. *Cell Tissue Res* 366:75–87.
15. Weed SA, Parsons JT (2001) Cortactin: Coupling membrane dynamics to cortical actin assembly. *Oncogene* 20:6418–6434.
16. Shimada T, et al. (2008) Shootin1 interacts with actin retrograde flow and L1-CAM to promote axon outgrowth. *J Cell Biol* 181:817–829.
17. Kubo Y, et al. (2015) Shootin1-cortactin interaction mediates signal-force transduction for axon outgrowth. *J Cell Biol* 210:663–676.
18. Rathjen FG, Schachner M (1984) Immunocytological and biochemical characterization of a new neuronal cell surface component (L1 antigen) which is involved in cell adhesion. *EMBO J* 3:1–10.
19. Kamiguchi H, Hlavin ML, Yamasaki M, Lemmon V (1998) Adhesion molecules and inherited diseases of the human nervous system. *Annu Rev Neurosci* 21:97–125.
20. Hu K, Ji L, Applegate KT, Danuser G, Waterman-Storer CM (2007) Differential transmission of actin motion within focal adhesions. *Science* 315:111–115.
21. Chan CE, Odde DJ (2008) Traction dynamics of filopodia on compliant substrates. *Science* 322:1687–1691.
22. Aratyn-Schaus Y, Gardel ML (2010) Transient frictional slip between integrin and the ECM in focal adhesions under myosin II tension. *Curr Biol* 20:1145–1153.
23. Mercurio AM (1990) Laminin: Multiple forms, multiple receptors. *Curr Opin Cell Biol* 2:845–849.
24. Colombo F, Meldolesi J (2015) L1-CAM and N-CAM: From adhesion proteins to pharmacological targets. *Trends Pharmacol Sci* 36:769–781.
25. Brümmendorf T, Rathjen FG (1996) Structure/function relationships of axon-associated adhesion receptors of the immunoglobulin superfamily. *Curr Opin Neurobiol* 6:584–593.
26. Hall H, Carbonetto S, Schachner M (1997) L1/HNK-1 carbohydrate- and beta 1 integrin-dependent neural cell adhesion to laminin-1. *J Neurochem* 68:544–553.
27. Esch T, Lemmon V, Banker G (1999) Local presentation of substrate molecules directs axon specification by cultured hippocampal neurons. *J Neurosci* 19:6417–6426.
28. Turney SG, Bridgman PC (2005) Laminin stimulates and guides axonal outgrowth via growth cone myosin II activity. *Nat Neurosci* 8:717–719.
29. Randlett O, Poggi L, Zolessi FR, Harris WA (2011) The oriented emergence of axons from retinal ganglion cells is directed by laminin contact in vivo. *Neuron* 70:266–280.
30. Chang S, Rathjen FG, Raper JA (1987) Extension of neurites on axons is impaired by antibodies against specific neural cell surface glycoproteins. *J Cell Biol* 104:355–362.
31. Cohen NR, et al. (1998) Errors in corticospinal axon guidance in mice lacking the neural cell adhesion molecule L1. *Curr Biol* 8:26–33.
32. Patzke C, Acuna C, Giam LR, Wernig M, Südhof TC (2016) Conditional deletion of L1CAM in human neurons impairs both axonal and dendritic arborization and action potential generation. *J Exp Med* 213:499–515.
33. Toriyama M, Kozawa S, Sakumura Y, Inagaki N (2013) Conversion of a signal into forces for axon outgrowth through Pak1-mediated shootin1 phosphorylation. *Curr Biol* 23:529–534.
34. Nichol RH, IV, Hagen KM, Lumbard DC, Dent EW, Gómez TM (2016) Guidance of axons by local coupling of retrograde flow to point contact adhesions. *J Neurosci* 36:2267–2282.
35. Itoh K, Fushiki S (2015) The role of L1cam in murine corticogenesis, and the pathogenesis of hydrocephalus. *Pathol Int* 65:58–66.
36. Yamasaki M, et al. (2011) Prenatal molecular diagnosis of a severe type of L1 syndrome (X-linked hydrocephalus). *J Neurosurg Pediatr* 8:411–416.
37. Jurado C, Haserick JR, Lee J (2005) Slipping or gripping? Fluorescent speckle microscopy in fish keratocytes reveals two different mechanisms for generating a retrograde flow of actin. *Mol Biol Cell* 16:507–518.
38. Hayashi S, et al. (2014) Protocadherin-17 mediates collective axon extension by recruiting actin regulator complexes to interaxonal contacts. *Dev Cell* 30:673–687.
39. Kiefel H, et al. (2012) L1CAM: A major driver for tumor cell invasion and motility. *Cell Adhes Migr* 6:374–384.